

## Effect of Lightning Impulse Current on The Grounding System Model

Nur Aqilah Sofiyah Hasni<sup>a</sup>, Syahrin Nizam Md Arshad@Hashim<sup>b</sup>, Sharin Ab Ghani<sup>c</sup>, Amizah Md Ariffen<sup>d</sup>, Wooi Chin Leong<sup>e</sup>, Muhammad Izuan Fahmi Romli<sup>f</sup>, Mohammed Imran Mousa<sup>g</sup>

<sup>a,b,d,e,f</sup> Centre of Excellent for Renewable Energy, Faculty of Electrical Engineering Technology, Universiti Malaysia Perlis (UniMAP), Perlis, Malaysia.

<sup>c</sup> Faculty of Electrical Engineering, Universiti Teknikal Malaysia Melaka, Melaka, Malaysia.

<sup>g</sup> Institute of High Voltage and High Current, School of Electrical Engineering, Faculty of Engineering, Universiti Teknologi Malaysia, Johor Bahru, Malaysia

**Article History:** Received: 10 January 2021; Revised: 12 February 2021; Accepted: 27 March 2021; Published online: 20 April 2021

**Abstract:** The main purpose of the grounding system is to protect human, electrical appliance and building from electrical shock due to lightning or another form of electricity that hazardous. Therefore, to achieve this goal, the fundamental part must be taken into account. In this paper, a different 3-D orientation of concrete has been designed using Comsol software to analyze the performance of the electric potential of the injected impulse in different cases and position of grounding system modelled. In this study, few grounding systems was modelled, which consist of Full concrete, Three-quarter concrete, Half concrete and A quarter concrete to analyse the electric potential of the injected lightning impulse current to the performance of the grounding system modelled. From the result obtained, full concrete was chosen as the best orientation of concrete to be employed at the grounding site. This is because, full concrete has the lowest electric potential value compared to the other cases and position of concrete..

**Keywords:**

### 1. Introduction

Lightning is a huge scale of electrostatic discharge (ESD). ESD occurs due to static charge build-up, which occurs by electrostatic induction or as a result of tribo-charging. Basically, the theory of ESD is the momentary flow of electrical energy between electrically charged bodies when in contact with each other (cloud to ground) [1]. Several Megavolts of voltage and tens of thousands of Ampere of current can be formed along the return stroke channel when lightning occurs [2]. Among the lightning types shows in **Figure 1**, namely cloud-to cloud, cloud-to-air, intra-cloud and cloud-to-ground, the most significant threat is the cloud-to-ground lightning [3][4]. 90% of cloud-to - ground lightning generates negative-current return strokes [5].

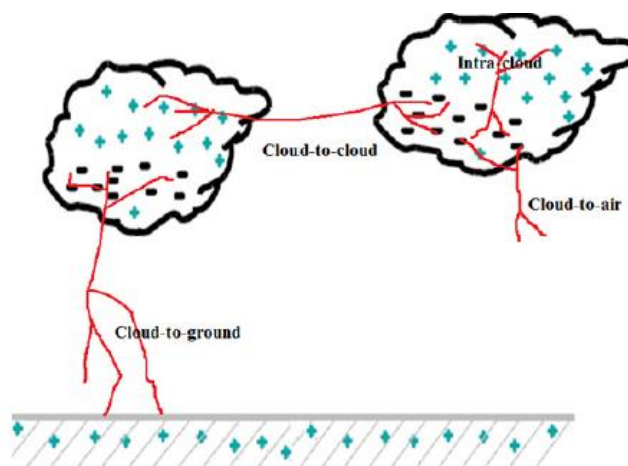


**Figure 1.** Different Types of Lightning Discharge [6]

Lightning-induced voltages, which may cause micro-interruption of the power supply or interruption of telecommunications or data-transmission networks during thunderstorms, have been seriously revisited due to increasing consumer demand for good power supply quality and reliability in the transmission of information [7]–[9]. A case recorded in Sweden in which, during a heavy thunderstorm, one high-voltage and several distribution transformers exploded, leaving 11000 people without electricity for 24 hours, is symptomatic of the imminent threat of lightning. This case illustrates that in a modern world, the disruption of information and electricity supplies may have significant consequences. Lightning also may cause damage to the electrical, communication or automation systems which can cost more than 250 million [10][11]. In the vicinity of a big hotel in Lausanne ,

Switzerland, a lightning stroke induced a voltage in the satellite antenna and damaged the TV sets in the building. [12].

Lightning is a natural phenomenon that has an incredible appearance and has always had a tremendous impact on humans and their communities due to its threats imposed on life and systems. With the growth of micro-electronics technology and the information industry, the loss caused by lightning stroke increased every year [13][14]. As the consequence, a grounding system with lightning research is develop in this study to recognize suited grounding system design that can endure severe thunderstorms better. In this study, few grounding systems with different position and size was modelled using software. The channel base current of the lightning stroke is the basis for analysing the distribution of electric potential. The lightning current is also used by many kinds of lightning models as an input feature since it is the source of electromagnetic fields [2]. The channel base current used in this study is Heidler Function model with waveshape of  $10/350\mu\text{s}$ ,  $2/70\mu\text{s}$ ,  $8/20\mu\text{s}$  and  $0.7/6\mu\text{s}$ . These different waveshape of Heidler model will be injected on the grounding system modelled and the distribution of electric potential of the injected impulse will be analyse.

## 2.The Grounding System Model

Numerical analysis is becoming a powerful approach to analyse the transient which is hard to solve by a conventional circuit-theory based approach. Nowadays, researchers and engineers tend to conduct numerical analysis techniques using computers for modelling and simulation, as it offers more effective and faster analysis [15].

The grounding system is modelled in 3 Dimension (3D) by using the Comsol Software. This grounding system modelled, consists of a copper rod, concrete with GEM and soil as shown in **Figure 2**. Copper is the most commonly used material for earth electrodes, due to its high conductivity and corrosion resistance [16]. A research study investigation by Halim et. al. found that the copper electrode is better than the galvanized steel electrode in term of lifespan or service life. Therefore, copper rod would be the best choice to be used in the project study in terms of the long-life materials [17]. In this experiment, copper rod with diameter of 0.014m and length of 2m had been used.

Furthermore, few grounding systems was modelled which consist of Full concrete, Three-quarter concrete, Half concrete and A quarter concrete to analyse the electric potential of the injected lightning impulse current to the performance of the grounding system modelled. Note that, the radius and length of the concrete in each grounding system modelled is different according to the cases that has been classified. Every position of concrete had been clarified into four different cases as shown in **Figure 3**. However, the volume of concrete for every cases and position are all the same which is 0.015404 meters<sup>3</sup>.

Then, a lightning impulse current using Heidler model with 4 different lightning current wave shapes was injected in this software to analyse the performance of the grounding system modelled. The Heidler model is chosen to be injected at the grounding system modelled because the equation is simple and Heidler model is widely used in EMTP/ATP computer program [18].

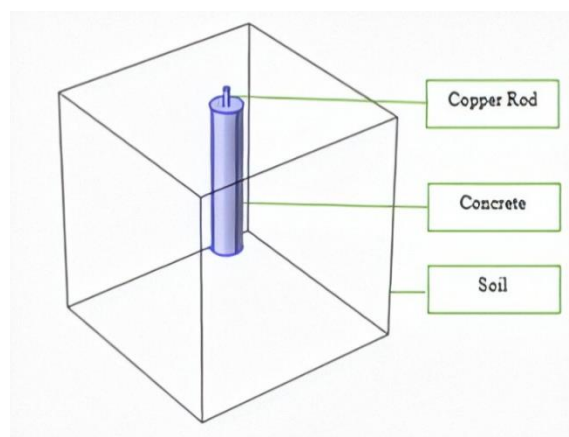


**Figure 2.** Grounding System Model.

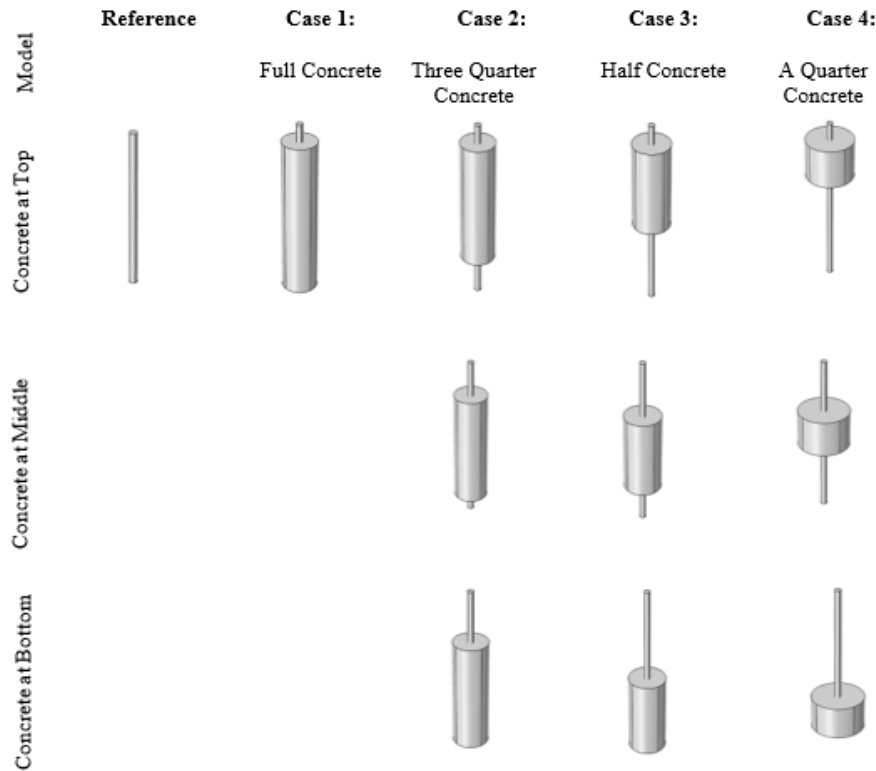


Figure 3. Different Orientation of Concrete.

2.1.Return Stroke Current at Base of The Channel

An analytical expression was adopted to represent the lightning current at the base of the return stroke channel, as proposed by Heidler. The Heidler function that was used in this study is defined in Equation 1 and 2 [19][20].

$$i(0,t) = \frac{i_0}{\eta} \frac{\left(\frac{t}{\tau_1}\right)^n}{1 + \left(\frac{t}{\tau_1}\right)^n} \exp\left(\frac{-t}{\tau_2}\right) \quad (1)$$

$$\eta = \exp\left[-\left(\tau_1 / \tau_2\right) \left(n \frac{\tau_2}{\tau_1}\right)^{\frac{1}{n}}\right] \quad (2)$$

2.2.Electric Potential Analysis

For electric potential analysis part, lightning impulse current using Heidler model was injected in this software [19]. Four lightning current waveshapes based on the Heidler function according to the standard current wave shapes (10/350 μs and 8/20μs) and non-standard wave shape (0.7/6 μs and 2/70 μs) had been used in this study. The parameters used were 31 kA of peak current **Table 1** shows the parameter for the channel base current modelled and presented in **Figure 4-7**.

Table 1. Lightning current wave shape parameters [10].

Lightning Current Wave shapes, $\mu\text{s}$	$\tau_1, \mu\text{s}$	$\tau_2, \mu\text{s}$	n
8/20	5.9	11.645	2
10/350	1	475	2
0.7/6	0.177	7	2
2/70	0.28	95	2

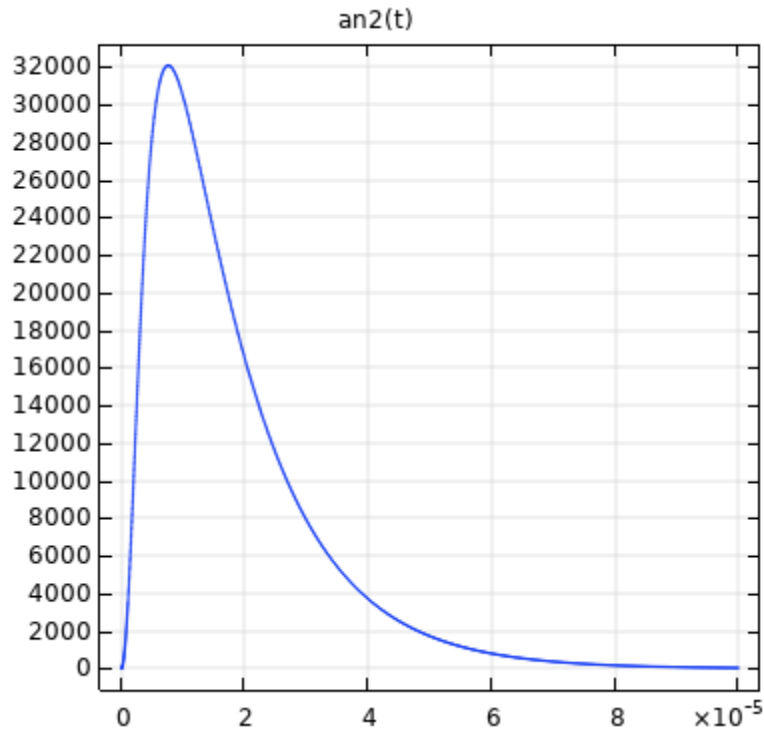


Figure 4. 8/20  $\mu\text{s}$  Waveform

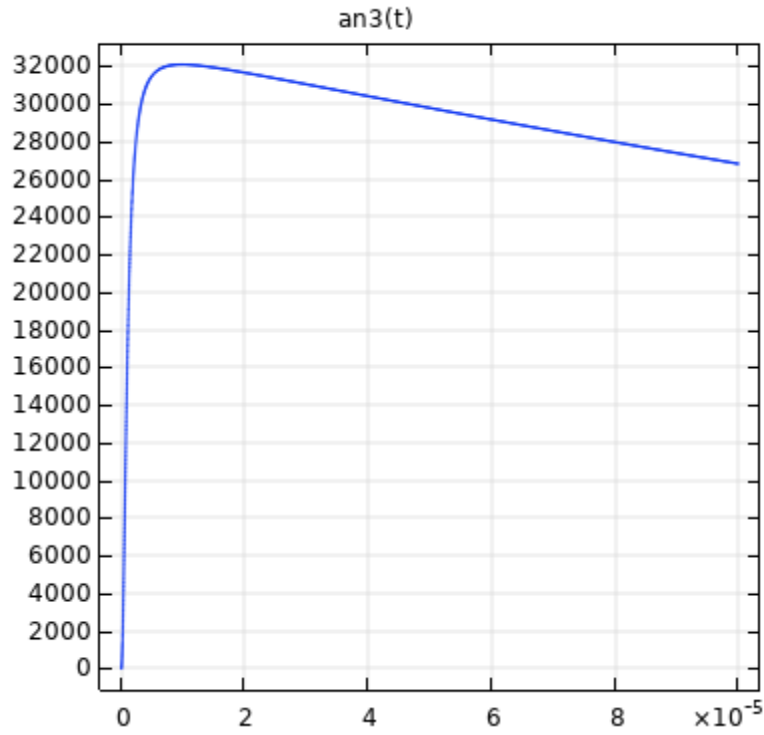


Figure 5. 10/350 $\mu$ s Waveform

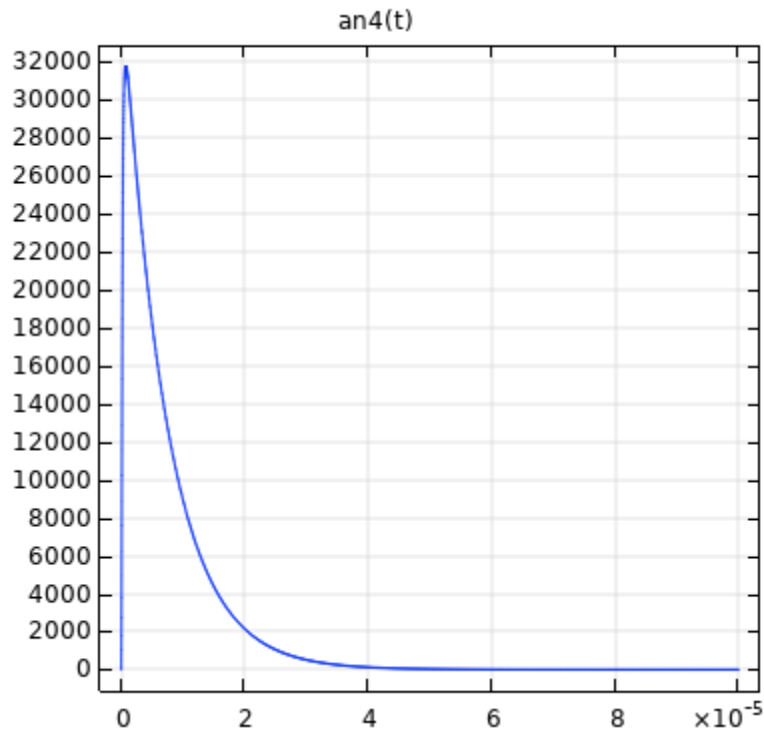


Figure 6. 0.7/6 $\mu$ s Waveform

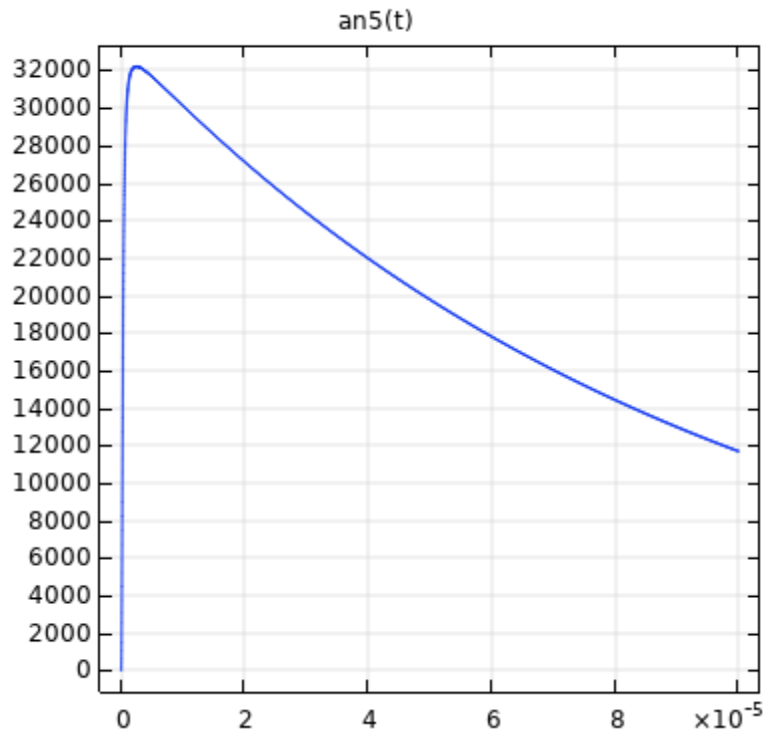


Figure 7. 2/70µs Waveform

Figure 8 shows a 3D Cut Point named Point 1. Point 1 is the selected area to analyse the electric potential value of the injected lightning impulse. Figure 9 shows the cut point at point 1 for all cases of concrete position.

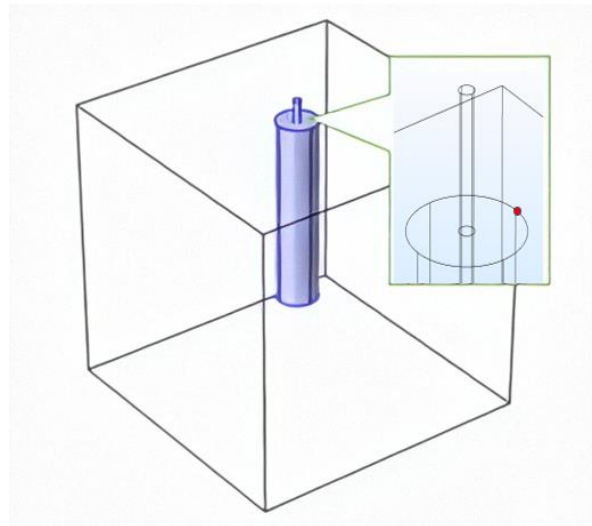
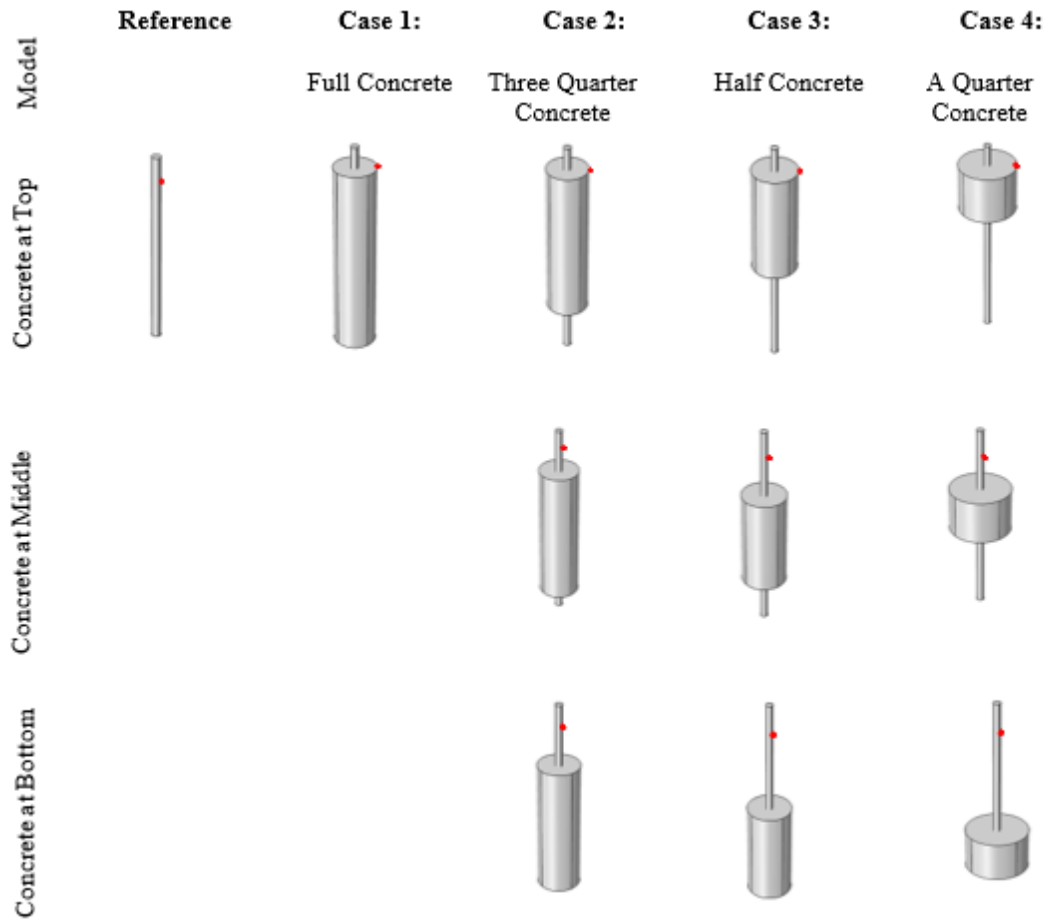


Figure 8. Cut Point at Point 1



**Figure 9.** The Cut Point at Point 1 for All Cases of Concrete Position

**3.Result and Discussion**

The highest electric potential value obtained from the injected lightning current waveshapes which consist of 8/20 $\mu$ s, 10/350 $\mu$ s, 0.7/6 $\mu$ s and 2/70 $\mu$ s is recorded and tabulated in **Table 2**.

**Table 2.** Result for All Grounding System Cases and Position

Model	Position	Lightning Current Wave shapes, $\mu$ s	Peak Voltage, V	Time, s
Reference Grounding System		8/20	5.984086	8.00E-06
		10/350	6.609668	1.00E-05
		0.7/6	6.723697	1.00E-06

		2/70	6.626634	3.00E-06
Case 1: Full Concrete		8/20	0.006934	8.00E-06
		10/350	0.007661	1.00E-05
		0.7/6	0.007794	1.00E-06
		2/70	0.00768	3.00E-06
Case 2: Three Quarter Concrete	Top	8/20	1.500115	8.00E-06
		10/350	1.657191	1.00E-05
		0.7/6	1.686186	1.00E-06
		2/70	1.661888	2.00E-06
	Middle	8/20	1.513955	8.00E-06
		10/350	1.672496	1.00E-05
		0.7/6	1.70126	1.00E-06
		2/70	1.676849	3.00E-06
	Bottom	8/20	1.502096	8.00E-06
		10/350	1.659433	9.00E-06



		0.7/6	1.688585	1.00E-06
		2/70	1.663626	3.00E-06
Case 3: Half concrete	Top	8/20	2.994656	8.00E-06
		10/350	3.305107	1.00E-05
		0.7/6	3.363005	1.00E-06
		2/70	3.314589	3.00E-06
	Middle	8/20	2.995932	8.00E-06
		10/350	3.309564	1.00E-05
		0.7/6	3.367516	1.00E-06
		2/70	3.318677	3.00E-06
	Bottom	8/20	2.991531	8.00E-06
		10/350	3.305643	1.00E-05
		0.7/6	3.363177	1.00E-06
		2/70	3.314679	3.00E-06
Case 4: A Quarter Concrete	Top	8/20	4.489577	8.00E-06

		10/350	4.953769	9.00E-06
		0.7/6	5.043605	1.00E-06
		2/70	4.968844	3.00E-06
	Middle	8/20	4.491756	8.00E-06
		10/350	4.963179	1.00E-05
		0.7/6	5.048882	1.00E-06
		2/70	4.975532	3.00E-06
	Bottom	8/20	4.486952	8.00E-06
		10/350	4.95637	1.00E-05
		0.7/6	5.042069	1.00E-06
		2/70	4.968524	3.00E-06

4.Overall Result

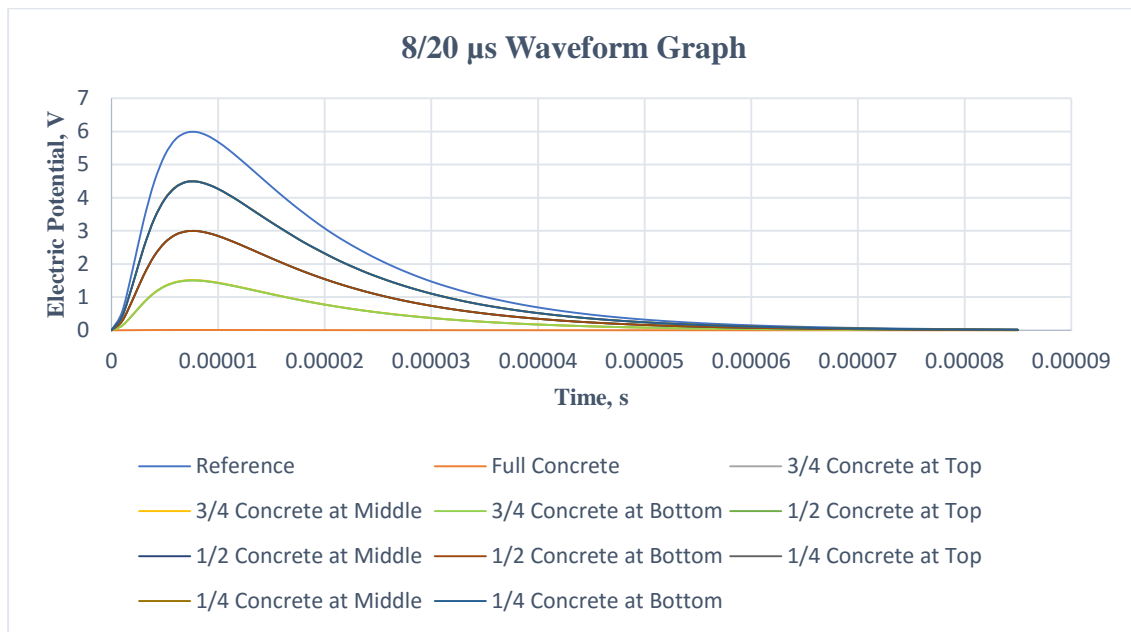
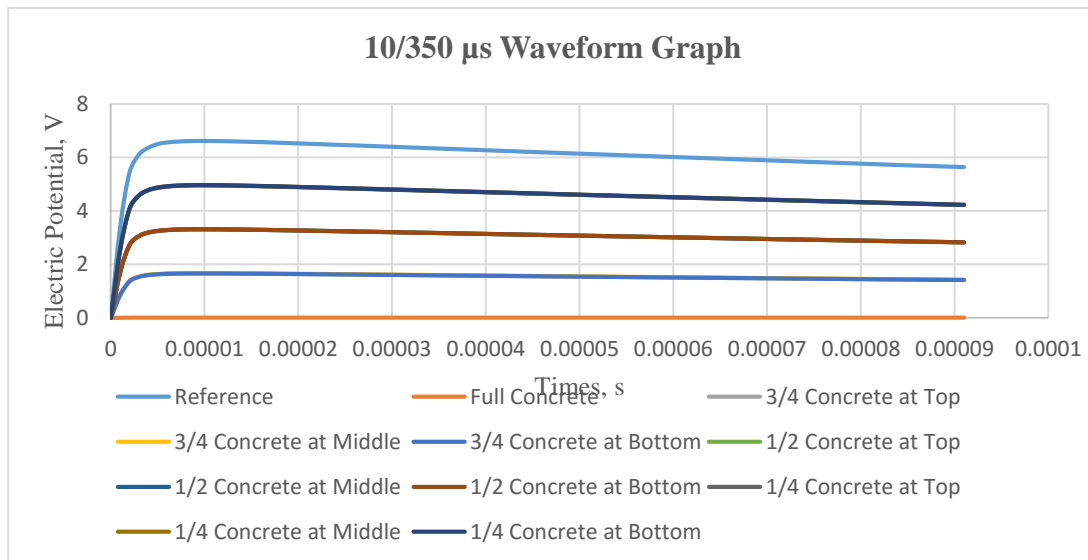


Figure 10. 8/20 μs Waveform for All Concrete Cases and Position

Table 3. Result for 8/20 μs Waveform for All Concrete Cases and Position

Concrete Cases and Position	Highest Time (s)	Percentage error (%)
Reference	5.984086	-
Full Concrete	0.006934	99.8841
3/4 Concrete at Top	1.500115	74.9316
3/4 Concrete at Middle	1.513955	74.7003
3/4 Concrete at Bottom	1.502096	74.8985
1/2 Concrete at Top	2.994656	49.9563
1/2 Concrete at Middle	2.995932	49.935
1/2 Concrete at Bottom	2.991531	50.0086
1/4 Concrete at Top	4.489577	24.9747
1/4 Concrete at Middle	4.491756	24.9383
1/4 Concrete at Bottom	4.486952	25.0186

According to Figure 10, all highest electric potential recorded are occurred at 0.000008 seconds uniformly for all cases and position of the grounding system modelled. From Table 3, Full concrete shows the highest percentage error with 99.8841% while 1/4 Concrete at Middle shows the lowest percentage error with 24.9383% to be compared to the reference grounding system. This is because full concrete is the most suitable concrete modelled that can withstand the 8/20 μs lightning waveform better compared to the others. The 1/4 Concrete at Middle is the most unsuitable grounding system modelled to withstand the 8/20 μs lightning waveform.



**Figure 11.** 10/350μs Waveform for All Concrete Cases and Position

**Table 4.** Result for 10/350μs Waveform for All Concrete Cases and Position

Concrete Cases and Position	Highest Time (s)	Percentage error (%)
Reference	6.609667875	-
Full Concrete	0.007660516	99.8841
3/4 Concrete at Top	1.657190667	74.9278
3/4 Concrete at Middle	1.672496463	74.6962
3/4 Concrete at Bottom	1.659432509	74.8939
1/2 Concrete at Top	3.305107384	49.9959
1/2 Concrete at Middle	3.309563506	49.9284
1/2 Concrete at Bottom	3.305642775	49.9878
1/4 Concrete at Top	4.95376857	25.0527
1/4 Concrete at Middle	4.963179251	24.9103
1/4 Concrete at Bottom	4.956369632	25.0133

According to **Figure 11**, all highest electric potential recorded are occurred at 0.00001 seconds for all cases and position of the grounding system modelled except 3/4 Concrete at Bottom and 1/4 Concrete at Top. The occurrence of the highest electric field of the injected impulse for both 3/4 Concrete at Bottom and 1/4 Concrete at Top is at 0.000009 seconds. From **Table 4**, Full concrete shows the highest percentage error with 99.8841% while 1/4 Concrete at Middle shows the lowest percentage error with 24.9103% to be compared to the reference grounding system. This result shows that 1/4 Concrete at Middle of grounding system is the least suitable concrete modelled to withstand the 10/350μs lightning waveform compared to the others grounding system modelled.

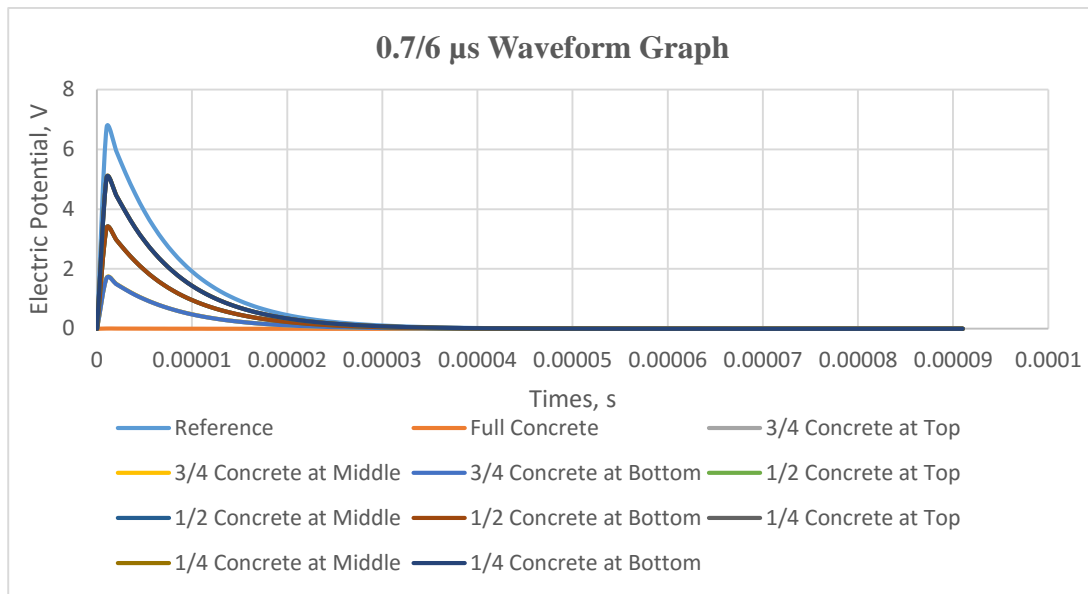


**Figure 12.** 0.7/6 $\mu$ s Waveform for All Concrete Cases and Position

**Table 5.** Result for 0.7/6 $\mu$ s Waveform for All Concrete Cases and Position

Concrete Cases and Position	Highest Time (s)	Percentage error (%)
Reference	6.723696703	-
Full Concrete	0.007793613	99.8841
3/4 Concrete at Top	1.686186405	74.9217
3/4 Concrete at Middle	1.701259618	74.6976
3/4 Concrete at Bottom	1.688585064	74.8861
1/2 Concrete at Top	3.363004709	49.9828
1/2 Concrete at Middle	3.367515806	49.9157
1/2 Concrete at Bottom	3.363177201	49.9802
1/4 Concrete at Top	5.043604914	24.9876
1/4 Concrete at Middle	5.048881746	24.9091
1/4 Concrete at Bottom	5.042068684	25.0105

According to **Figure 12**, all highest electric potential recorded are occurred at 0.000001 seconds uniformly for all cases and position of the grounding system modelled. From **Table 5**, Full concrete shows the highest percentage error with 99.8841% while 1/4 Concrete at Middle shows the lowest percentage error with 24.9061% to be compared to the reference grounding system. This is because full concrete is the most suitable concrete modelled that can withstand the 0.7/6 $\mu$ s lightning waveform better compared to the others.

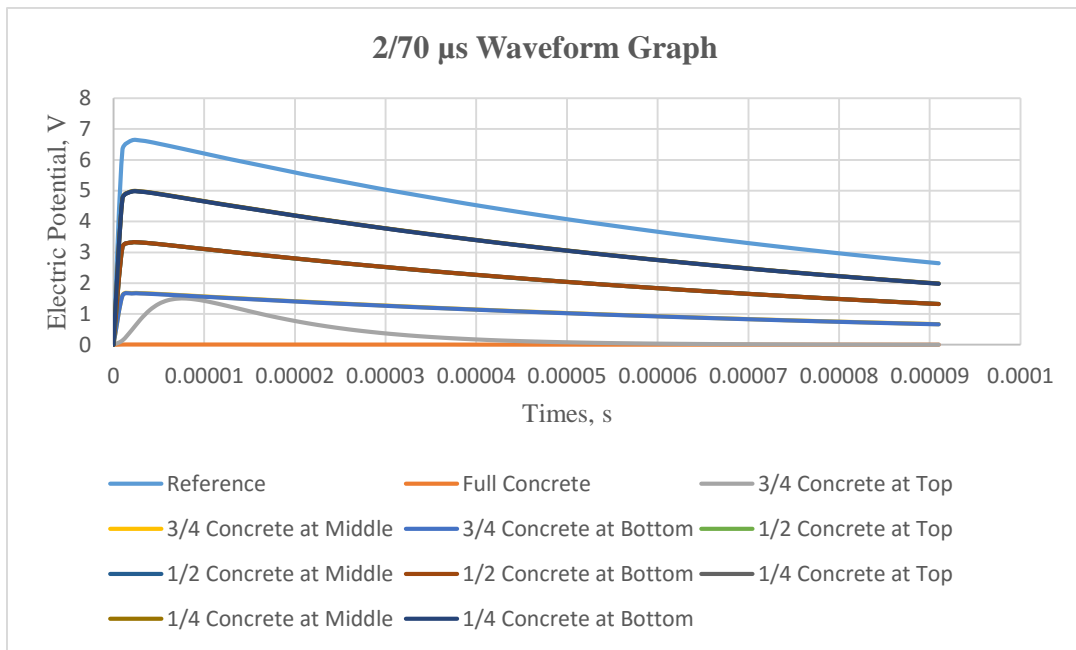


Figure 13. 2/70μs Waveform for All Concrete Cases and Position

Table 6. Result for 2/70μs Waveform for All Concrete Cases and Position

Concrete Cases and Position	Highest Time (s)	Percentage error (%)
Reference	6.626633961	
Full Concrete	0.007680115	99.8841
3/4 Concrete at Top	1.500115228	77.3623
3/4 Concrete at Middle	1.676849219	74.6953
3/4 Concrete at Bottom	1.663626027	74.8949
1/2 Concrete at Top	3.314589266	49.9808
1/2 Concrete at Middle	3.318677468	49.9191
1/2 Concrete at Bottom	3.314678514	49.9795
1/4 Concrete at Top	4.96884373	25.0171
1/4 Concrete at Middle	4.975531558	24.9162
1/4 Concrete at Bottom	4.968523724	25.0219

According to Figure 13, all highest electric potential recorded are occurred at 0.00001 seconds for all cases and position of the grounding system modelled except 3/4 Concrete at Top. The occurrence of the highest electric field of the injected impulse for 3/4 Concrete at Bottom is at 0.000008 seconds. From Table 6, Full concrete shows the highest percentage error with 99.8841% while 1/4 Concrete at Middle shows the lowest percentage error with 24.9162% to be compared to the reference grounding system. This is because full concrete is the most suitable concrete modelled to withstand the 2/70μs lightning waveform.

Therefore, from the overall result, case 1 which is full concrete is the best orientation of concrete compared to the other cases and position. This is because full concrete shows the best performance in terms of the lowest electric potential at point 1. Moreover, full concrete is the common grounding system model used according to the previous recent year study. In 2015, a 2D full concrete grounding system was designed to coat the electrode by using COMSOL Software to investigate the grounding system with additive and without additive material [21]. Also in year 2018, a full concrete filled with additive material has been used by N.H. Halim to investigate the

performance of galvanized steel and copper electrode using paddy husk ashes [17]. Therefore, full concrete is the best grounding system model to be install in the grounding site.

## 5. Conclusion

From the result obtained, it is clearly showing that case 1 which is full concrete shows the stable line graph with the lowest electric potential compared to the other grounding system modelled. This is followed by a grounding system with three-quarter concrete, half concrete and a quarter concrete. The Reference grounding system showed the highest electric potential compared to the other grounding systems.

An excellent grounding system must be able to provide the lowest impedance path to the ground. According to Ohm's Law, lower in electric potential value will lower the resistance value. Therefore, full concrete is the most suitable grounding system modelled to be installed at the grounding site as it performed the best in terms of the lowest electric potential.

## 6. Acknowledgments

Authors wishing to acknowledge assistance or encouragement from colleagues, special work by technical staff or financial support from FRGS (ref. no. RACER/1/2019/TK04/UNIMAP//1)

### 1. References

2. M. L. Akinyemi, A. O. Boyo, M. E. Emetere, M. R. Usikalu, and F. O. Olawole, "Lightning a Fundamental of Atmospheric Electricity," *IERI Procedia*, vol. 9, pp. 47–52, 2014, doi: 10.1016/j.ieri.2014.09.039.
3. Y. Chen, S. Liu, X. Wu, and F. Zhang, "A new kind of lightning channel-base current function," *IEEE Int. Symp. Electromagn. Compat.*, vol. 2002-Janua, no. 1, pp. 304–307, 2002, doi: 10.1109/ELMAGC.2002.1177430.
4. V. Cooray, *An introduction to lightning*. 2015.
5. S. N. M. Arshad, "The human body," *Am. J. Surg.*, vol. 38, no. 2, p. 409, 1937, doi: 10.1016/s0002-9610(37)90465-3.
6. M. I. Mousa, Z. Abdul-Malek, and M. R. M. Esa, "Effects of return stroke parameters and soil water content on EMF characteristics," *Appl. Comput. Electromagn. Soc. J.*, vol. 34, no. 8, pp. 1219–1225, 2019.
7. V. A. Rakov, "Lightning Phenomenology and Parameters Important for Lightning Protection," 2007 Int. Symp. Light. Prot. IX SIPDA, no. November, 2007, [Online]. Available: <http://ws9.iee.usp.br/sipdax/papersix/sessao12/12.1.pdf>.
8. F. M. Tesche et al., "Estimates of lightning-induced voltage stresses within buried shielded conduits," *IEEE Trans. Electromagn. Compat.*, vol. 40, no. 4 PART 2, pp. 492–504, 1998, doi: 10.1109/15.736209.
9. M. G. Sorwar, H. Ahmad, and M. M. Ali, "Analysis of transients in overhead telecommunication subscriber line due to nearby lightning return stroke," *IEEE Int. Symp. Electromagn. Compat.*, vol. 2, pp. 1083–1088, 1998, doi: 10.1109/isemc.1998.750359.
10. M. Ishii, K. Michishita, and Y. Hongo, "Experimental study of lightning-induced voltage on an overhead wire over lossy ground," *IEEE Trans. Electromagn. Compat.*, vol. 41, no. 1, pp. 39–45, 1999, doi: 10.1109/15.748135.
11. M. S. M. Nasir, M. Z. A. Ab-Kadir, M. A. M. Radzi, M. Izadi, N. I. Ahmad, and N. H. Zaini, "Lightning performance analysis of a rooftop grid-connected solar photovoltaic without external lightning protection system," *PLoS One*, vol. 14, no. 7, pp. 1–19, 2019, doi: 10.1371/journal.pone.0219326.
12. S. N. M. Arshad et al., "Analysis behavior of soil resistivity profiling base on UniMAP condition," *J. Phys. Conf. Ser.*, vol. 1432, no. 1, 2020, doi: 10.1088/1742-6596/1432/1/012038.
13. M. O. Goni, E. Kaneko, and A. Ametani, "Simulation of lightning return stroke currents and its effect to nearby overhead conductor," *Appl. Comput. Electromagn. Soc. J.*, vol. 24, no. 5, pp. 469–477, 2009.
14. M. Stolzenburg and T. C. Marshall, *Electric field and charge structure in lightning-producing clouds*. 2009.
15. W. Sima, P. Sun, M. Yang, J. Wu, and J. Hua, "Impact of time parameters of lightning impulse on the breakdown characteristics of oil paper insulation," *High Volt.*, vol. 1, no. 1, pp. 18–24, 2016, doi: 10.1049/hve.2016.0009.
16. H. Z. Quanzhong Huang, Guanhua Huang, "A finite element solution for the fractional advection–dispersion equation," p. 12, 2008.
  - A. Ahmad, M. R. A. Saroni, I. A. W. A. Razak, and S. Ahmad, "A case study on ground resistance based on copper electrode vs. galvanized iron electrode," *Conf. Proceeding - 2014 IEEE Int. Conf. Power Energy, PECon 2014*, no. October, pp. 406–410, 2014, doi: 10.1109/PECON.2014.7062479.

17. S. N. M. Arshad, N. S. Tajudin, N. H. Halim, A. Z. Abdullah, C. L. Wooi, and N. Hussin, "Grounding Electrodes Using Paddy Husk Ash as An Additive Material to Grounding System," 2018 IEEE 7th Int. Conf. Power Energy, pp. 283–287, 2018.
18. J. Furgał, "Influence of lightning current model on simulations of overvoltages in high voltage overhead transmission systems," *Energies*, vol. 13, no. 2, 2020, doi: 10.3390/en13020296.
19. F. Rachidi et al., "Current and electromagnetic field associated with lightning-return strokes to tall towers," *IEEE Trans. Electromagn. Compat.*, vol. 43, no. 3, pp. 356–366, 2001, doi: 10.1109/15.942607.
20. C. L. W. and N. H. N.S. Tajudin, N.H. Halim, A.Z. Abdullah, "Underground Cable by using Alternative Transients Program / Electromagnetic Transients Program," 2018 IEEE 7th Int. Conf. Power Energy, pp. 209–214, 2018.
  - A. Memon, "Modelling Single Grounding Electrode Using Comsol," no. June, 2015.